Thermal Fatigue of Pressurized Water Reactor Coolant System Loop Drain Lines Due to Outflow Activities

Yue Zou[1]
Dominion Energy,
Richmond, VA 23060;
Department of Mechanical and
Nuclear Engineering,
Virginia Commonwealth University,
Richmond, VA 23284
e-mail: yue.zou@dominionenergy.com

Brian Derreberry
Dominion Energy,
Richmond, VA 23060
e-mail: Brian.derreberry@dominionenergy.com

Thermal cycling induced fatigue is widely recognized as one of the major contributors to the damage of nuclear plant piping systems, especially at locations where turbulent mixing of flows with different temperature occurs. Thermal fatigue caused by swirl penetration interaction with normally stagnant water layers has been identified as a mechanism that can lead to cracking in dead-ended branch lines attached to pressurized water reactor (PWR) primary coolant system. Electric Power Research Institute (EPRI) has developed screening methods, derived from extensive testing and analysis, to determine which lines are potentially affected as well as evaluation methods to perform evaluations of this thermal fatigue mechanism for the U.S. PWR plants. However, recent industry operating experience (OE) indicates that the model used to predict thermal fatigue due to swirl penetration is not fully understood. There are limitations with the EPRI generic evaluation. In addition, cumulative effects from other thermal transients, especially those resulted from outflow activities, may also contribute to the failure of reactor coolant system (RCS) branch lines. In this paper, we report direct OE from one of our PWR units where thermal fatigue cracking is observed at the RCS loop drain line close to the welded region of the elbow. A conservative analytical approach that takes into account the influence of thermal stratification, in accordance with ASME section III class 1 piping stress method, is also proposed to evaluate the severity of fatigue damage to the RCS drain line, as a result of various transients, particularly the transients from outflow activities. Finally, recommendations are made for future operation and inspection based on results of the evaluation. [DOI: 10.1115/1.4053013]

1 Introduction

Thermal fatigue caused by swirl penetration interaction with normally stagnant water layers has been identified as a mechanism that can lead to cracking in dead-ended branch lines attached to pressurized water reactor (PWR) primary coolant piping. The Electric Power Research Institute (EPRI) has developed screening methods to determine which lines are potentially affected as well as evaluation methods to perform evaluations of this thermal fatigue mechanism [1–4]. These methods are published under the EPRI material reliability program (MRP) for managing the effects of aging degradation in PWR internals. EPRI Report MRP-132 [1] summarizes the screening and evaluation methodology derived from extensive testing and analysis, including its application in a generic assessment of thermal cycling and fatigue in U.S. PWR plants. EPRI Report MRP-146 [2] provides guidance for the application of the assessment techniques in MRP-132 [1] and guidance relative to actions that can be taken based on the results of the assessments. The EPRI screening methods have been performed on the reactor coolant system (RCS) loop drain lines for North Anna (NAPS) and Surry (SPS) power stations. Six down horizontal (DH) lines at NAPS, all off RCS cold legs, were screened-in to be susceptible to thermal cycling by MRP-170 (Palo Alto, CA) [3] evaluations. These lines were then evaluated by the MRP-146S [4] generic evaluation and concluded that thermal fatigue was NOT significant. The RCS loop drain lines at SPS were all screened-out by MRP-170 [3] evaluations. It should be noted that there are limitations with MRP-146/MRP-146S [2,4] generic evaluation: it does not apply to lines with socket welded fittings and is also limited to the piping sizes/geometry of DH lines; it also does not include cumulative effects from various thermal transients that result from reactor services, such as the RCS chemistry sampling activities and excess letdown. These transients can result in further thermal fatigue damage to the DH line elbow, where stress concentrators occur when hot flow passes through the drain lines that are normally at ambient conditions.

On Dec. 22, 2014, a nonisolable RCS pressure boundary leak was identified on the North Anna Unit 1 "B" cold leg drain line upstream of the isolation valve. A through-wall axial crack was identified in the elbow region along with circumferential cracks in the welded region. Follow-up material inspections determined that the cracks were thermal fatigue related. Recently, several operating experiences (OE) have been reported across the industry [5]: MRP-85, material reliability program: operating experience regarding thermal fatigue of piping connected to PWR reactor coolant systems, documents 22 cracking events associated with thermal fatigue. Of the 22 events, 14 have been leakage incidents in nonisolable portions of normally stagnant piping systems connected to the RCS and two were leakage in isolable portions. Also, there were six part-through-wall cracking incidents in nonisolable piping due to thermal fatigue. Oconee nuclear power station also experienced a failure of a 50-mm (2-in) loop drain line due to thermal fatigue. A contributing cause to this event was the chemistry samples that had been collected from the same line. Although this OE was in the Institute of Nuclear Power Operations database and was discussed in MRP-85, evaluation of the additional stress caused by sampling was not clearly mentioned or referenced in associated EPRI guidance. In this article, we discuss in detail on the findings of the OE from dominion energy's own fleet nuclear stations through material examinations. In addition, an evaluation method for thermal fatigue is proposed to evaluate damages as a result of various transients that are not considered in the MRP generic evaluation.

The ASME piping stress formula is widely adopted across the industry for pipe integrity evaluations. Evaluating thermal fatigue

[1]Corresponding author.

Manuscript received February 7, 2021; final manuscript received November 3, 2021; published online May 26, 2022. Assoc. Editor: Asif Arastu.

with this method requires precise cycle counting as well as thermal load determination. Transients involving hot and cold fluid entering each other may cause thermal stratification, resulting in thermal bending stresses in addition to regular thermal loads. Seo et al. and Kweon et al. [6,7] have investigated the fatigue effect of thermal stratification on a safety injection line using ASME class 1 formula along with finite element thermal analysis. We present, in this article, an analytical approach with reasonable assumptions to address the thermal bending due to thermal stratification. Previously, the European Commission [8] has also suggested the feasibility of performing fatigue assessment on thermal stratification using ASME method [9]. It is the purpose of this article to focus on the influence of various transients, particularly those as a result of outflow activities such as chemistry sampling and excess letdown, on thermal fatigue of the RCS drain lines. A reliable evaluation method is needed to provide a basis for understanding the severity of different transients, which can not only assist the plant operation but also reduce time-loss resulted from unplanned outages.

2 Design Information

North Anna power station has two Westinghouse three-loop design pressurized water reactors, each with a capacity of around 900 MW. The NAPS Unit 1 was constructed in 1971 and began commercial operation in May 1978. The NAPS unit 1 reactor coolant system has three steam generators (SG) with three reactor coolant pumps (RCPs). Each RCS loop consists of a hot leg prior to each SG and a cold leg after each SG. Each loop drain line (50 mm or 2 in. in diameter) taps off the bottom of the RCS cold leg between the RCP and SG and drops down and turns 90 deg via an elbow to the horizontal, as shown in the picture of Fig. 1. The loop drain lines are then routed to excess letdown and RCS sample lines. All three drains have a vertical run dropping approximately 340 mm (13.5 in.) from the bottom of the RCS piping to the centerline of the elbow, and a horizontal run extending 1070 mm (3 ft 6 in.) to the first isolation valve. The 50-mm (2-in.) line is schedule 160 A376-Type-316 stainless steel pipe that is butt welded to the RCS nozzle and then drops 350 mm (13 3/4 in.) down. It then transitions to a 50-mm (2-in.) 90-deg schedule 160 A403-WP-316 stainless steel elbow which is butt welded on both sides. The line then travels horizontally another 760 mm (2 ft 6 in.) to a "T" where it is diverted between the sample system line and the excess letdown line. SPS is a similar plant to NAPS. However, the RCS loop drain line configuration of SPS is slightly different from that of NAPS: it has a much longer vertical drop from the RCS line; the transition connection of the RCS loop drain line from vertical to horizontal is through a socket weld rather than butt weld.

Chemistry sampling is performed by purging to gas stripper. During the reactor coolant sampling process, flow at elevated temperature is introduced into the drain line and then exits from a 20-mm (3/4-in.) sampling line, which is usually located at a close vicinity to the DH line elbow as shown and illustrated in Fig. 1. The RCS sampling is conducted at a flow rate of 0.18–0.23 m^3/h (0.8 to 1±0.01 gpm) and can occur when the reactor is online or offline, corresponding to different coolant temperatures. From 2004 and through 2014, both NAPS and SPS units had begun conducting chemistry sampling while the reactors were online. Around 500 sampling had been documented on a single loop during the 10-year period.

In contrast, the excess letdown is a more severe transient with a flow rate of 3.4–4.8 m^3/h (15 to 21±0.2 gpm) and a temperature changes from 50 to 286 °C (120 to 547±2 °F) in 14.6 s. The maximum temperature during excess letdown can last for about a one-hour in duration. In addition, it is conducted by passing fluid through the entire RCS drain line (off cold leg) as opposed to the sampling line. However, the excess letdown is conducted at a much less frequency of only a few times per year. Thermal stratification may occur during chemistry sampling activities, as hot flow enters the stagnant coolant existing in the drain lines, causing further damage due to additional bending stresses. The associated thermal transients with various flow paths and conditions result in different stress ranges that contribute to overall thermal fatigue damages.

3 Material Inspection

The as-received elbow with the attached downstream section of approximately 300 mm (12 in.) of pipe was cleaned in a tank of P&G™ water to remove as much loose contamination as possible. The downstream section of pipe was cut at the elbow longitudinally to allow inspection of the interior surface. A through-wall axial crack about 50 mm (2 in.) long was identified approximately 25 mm (1 in.) from the weld on the pipe side of weld. The elbow was sectioned in half longitudinally to allow inspection of the interior surface. A through-wall axial crack about 50 mm (2 in.) long was identified in the elbow, along the inside diameter of the pipe section. Circumferentially oriented cracks about 20 mm (0.75 in.) long were also identified in the toe of the weld region on both the pipe and elbow sides of the circumferential weld. Dye penetrant was applied to the elbow to enhance the crack location for photographing. Cross-sections were cut from the elbow through the crack approximately 25 mm (1 in.) from the leak location as well as from the downstream weld for metallography, as shown in Fig. 2. Some branching of the crack had occurred along the end away from the weld. It is also noticed that the fracture surface of the sample was heavily oxidized, indicating long-term exposure in

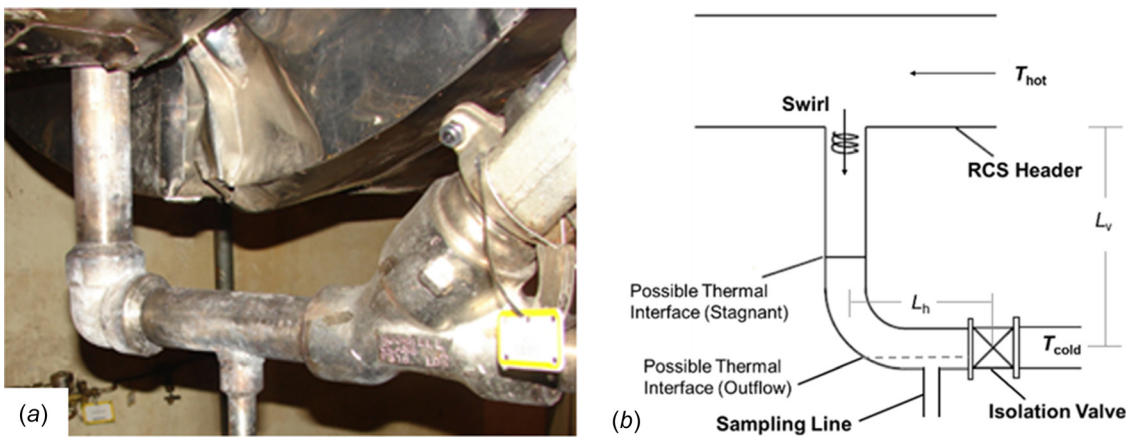

Fig. 1 (*a*) A photo of the RCS loop drain line down horizontal elbow with sampling line and isolation valve and (*b*) a schematic diagram of the RCS loop drain line down horizontal elbow and thermal cycling mechanism

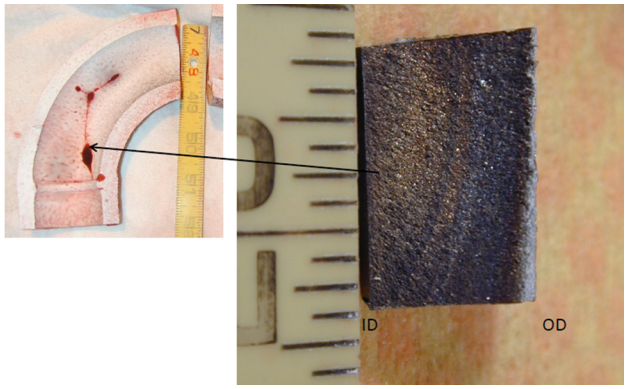

Fig. 2 Photo of a section of the crack that was cut out and opened in lab, showing heavily oxidized fracture surface

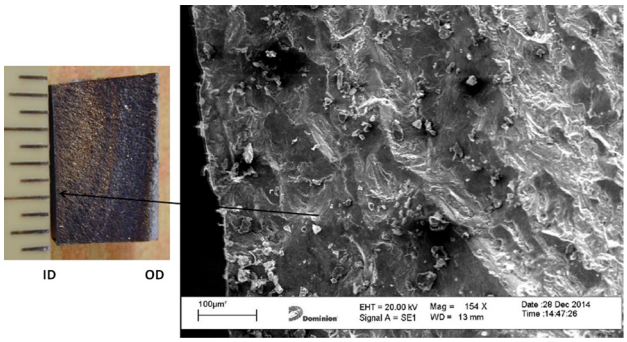

Fig. 3 SEM micrograph taken from the opened crack face near the ID, showing worn transgranular fracture (original magnification 154×)

the RCS environment. The samples were then polished to a 1-μm finish using standard metallographic techniques and then etched electrolytically with 10% oxalic acid to reveal the grain structure of the material.

A section of the crack shown in Fig. 2 as indicated by the arrow was cut out and opened in lab for fractographical examination. Three locations of the cutout sample from near the origin of the crack (close to ID), the center of the crack face, and the leading edge of the crack (close to OD) were examined using scanning electron microscope (SEM). Figure 3 shows a SEM micrograph of the fracture surface, close to the pipe inside surface, that appears to have worn transgranular fracture. The transgranular fracture becomes more well-defined at the center of the crack face as shown in Fig. 4. This cracking feature is more pronounced toward the crack tip because of less exposure in the RCS environment.

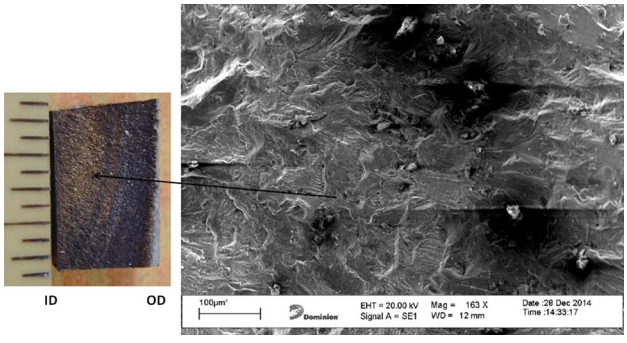

Fig. 4 SEM micrograph taken from approximately the center of the crack face, showing more well-defined transgranular fracture (original magnification 163×)

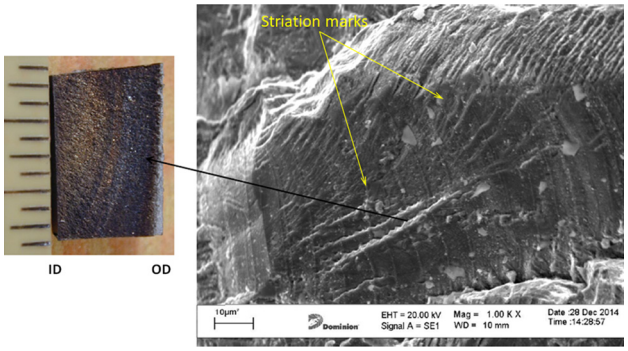

Fig. 5 SEM micrograph showing the surface features along the leading edge of the crack. The surface has very faceted transgranular appearance with some large striation-like marks across it. Original magnification 1000×.

The SEM micrograph of the fracture surface along the leading edge of the axial crack in Fig. 5 clearly shows that the fracture surface has very faceted transgranular appearance. Large striation-like marks were noticed across the surface, indicating possible thermal fatigue related failure during the crack propagation. Further investigation showed finer striation marks with a spacing around 7 μm.

To determine a comprehensive and direct cause of the thermal fatigue failure in the loop drain line, a failure modes and effects analysis (FMEA) was performed and revealed two main contributors to this failure: swirl penetration and chemistry sampling. Other degradation mechanisms that were considered but discounted include the following: stress corrosion cracking, general corrosion, and flow accelerated corrosion. Stress corrosion cracking is not a concern at this location since it is in direct contact with the RCS, which utilizes a chemistry control program to ensure known contaminants such as chlorides, fluorides, and sulfates are maintained below required levels. General corrosion is not a concern because the drain line is constructed of stainless steel which is not susceptible to general corrosion. Flow accelerated corrosion seldom occurs in stainless steel and is not considered relevant at this location because the line is primarily stagnant. As a matter of fact, outflow activities can induce thermal transients to the drain line depending on the flow path and the flow conditions, such as temperature, pressure, and velocity. In the following section, we evaluate outflow and plant operation activities to better understand how different transients contribute to the overall fatigue utilization.

4 Analysis Method

4.1 Modeling Description. A piping model of the RCS loop as well as the drain lines attached to it was constructed using NUPIPE-II computer code. The full RCS loop was modeled to investigate the impact of plant operation to the loop drain line, including steady-state power fluctuation, reactor startup and shutdown, and pressurizer heat-up and cooldown etc. An isometric sketch of the loop drain line is presented in Fig. 6. The basic method of analysis used in NUPIPE-II is the finite element stiffness method. In accordance with this method, the continuous piping is mathematically idealized as an assembly of elastic structural members connecting discrete nodal points. Nodal points are placed in such a manner as to isolate particular types of piping elements, such as straight runs of pipe, elbows, valves, etc., for which force-deformation characteristics can be categorized. Nodal points are also placed at all discontinuities, such as piping supports, concentrated weights, branch lines and changes in cross section. System loads, such as weights are applied at the nodal points. Stiffness characteristics of the interconnecting members are related to the effective shear area and moment of inertia of the

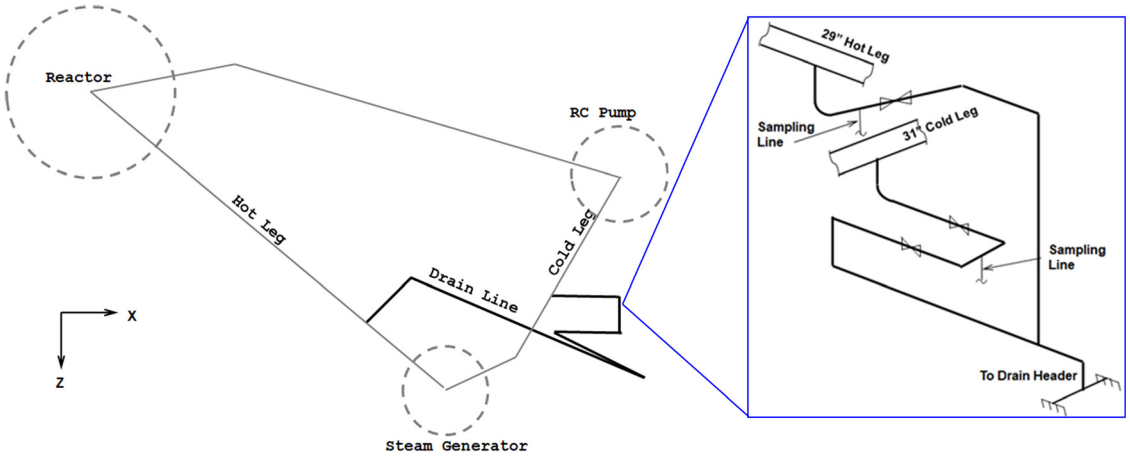

Fig. 6 Top view of the RCS loop with the loop drain lines (bold) attached to it, showing the piping route with respect to the reactor, the reactor coolant pump, and the steam generator, with an Isometric sketch of the RCS loop drain line configuration

pipe. The 50-mm (2-in.) RCS loop drain lines are then conservatively evaluated using the ASME code section III class 1 piping stress formula and criteria (NB-3600) [9], consisting of membrane, bending, pipe through-wall thermal gradients, and gross discontinuity terms.

4.2 Thermal Stratification. Thermal stratification may occur as hot RCS fluid enters the drain line and mixes with the cold (ambient temperature) stagnant coolant. When thermal stratification occurs, the pipe is partially filled with hot water and partially filled with cold water. In some cases, the interface is very small, and the gradient is very large; while in the other extreme, the transition between the hot and cold fluid can occur over the entire pipe cross section [10], as illustrated by Fig. 7. The causes of each of these two cases are related in a complex fashion to the flow rate, temperature difference, length of flow, pipe slope, pipe material and temperature (insulation characteristics), entrance conditions, and exit conditions. Once the interface height has been identified, the velocity and other fluid parameters can be calculated for given volumetric flow rates. This is important because calculation of the heat transfer and stability of a stratified flow is dependent on the flow velocity.

A simple methodology has been provided in Ref. [10] to estimate the interface height of a stratified flow by assuming that the interface is well defined, that is, no intermixing layer. A diagram is included in Fig. 8 for illustration of this method. The stratified flow interface height is calculated using an iterative solution of the equation described as follows:

$$Q^2 = \frac{\Delta\rho}{\rho} \cdot \frac{gA_y{}^3}{W_y} \tag{1}$$

where Q is the volumetric flow rate, A_y is flow area, and W_y is width of free surface. By plugging in $A_y = d^2 \cdot (\alpha_y - \sin\alpha_y)/8$ and

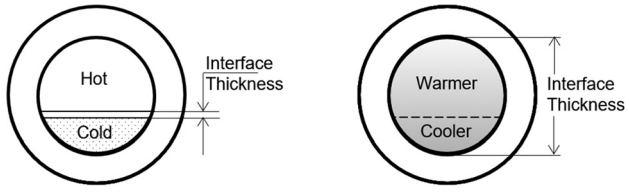

Fig. 7 Illustration of thermal stratification with hot and cold fluid within a pipe section, showing thin versus intermixing over the entire cross section

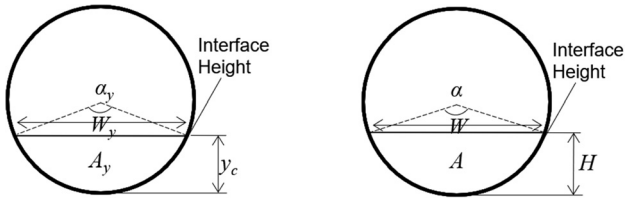

Fig. 8 Illustration of stratification interface height

$W_y = d \cdot \sin(\alpha_y/2)$, and by re-arranging the terms, the equation can be written as

$$\frac{\sin(\alpha_y/2)}{(\alpha_y - \sin\alpha_y)^3} = \frac{\Delta\rho}{\rho} \cdot \frac{gd^5}{512Q^2} \tag{2}$$

where d is the pipe inside diameter, ρ is the density of the flowing fluid, $\Delta\rho$ is the absolute value of the density difference between stratified fluids, and g is the acceleration due to gravity. The angle α_y bounding the critical depth in radians can be solved from the relation above for given flow properties. The critical depth is calculated as $y_y = d(1 - \cos(\alpha_y/2))/2$. The stratified interface height, H, can then be determined based on flow condition, pipe configuration, flow entrance, and exit conditions in accordance with Table 3.1–1 of Ref. [10]. Note that the pipe Richardson number, $\mathbf{Ri_p} = (\Delta\rho/\rho) \cdot (gd/u^2)$ (u is average velocity of the stratified flowing fluid), must be calculated to verify that the flow will remain stratified. If $\mathbf{Ri_p}$ is less than 4.0, it can be assumed that stratification will not occur in the pipe, which is equivalent to if the height is calculated to be greater than $0.83d$ for horizontal pipes.

Because the sampling line at the loop drain off the hot leg is located fairly close to the DH elbow (within 30 cm), it is less likely that thermal stratification would occur (i.e., hot flow exits downward through the sampling line right after it passes the DH elbow). The sampling line at the loop drain off the cold leg, however, is located much further away from the DH elbow, thus, providing adequate range for the flow to remain stratified if thermal stratification would have occurred according to the method described in this section. It is calculated that the excess letdown flow will not remain stratified due to high volumetric flow rate, while the chemistry sampling flow from the cold leg loop drain is expected to stratify with an interface located close to the midsection of the loop drain pipe, as summarized in Table 1. This will result in bending moments in addition to thermal expansion loads.

Table 1 Predicted thermal stratification condition for excess letdown and RCS sampling

	Stratified height to diameter ratio	Richardson number	Stratification condition
Outflow activity transients	H/d	Ri_p	Y/N
Excess letdown	1.00	0.02	N
Online chemistry sampling	0.40	10.13	Y
Offline chemistry sampling	0.70	4.58	Y

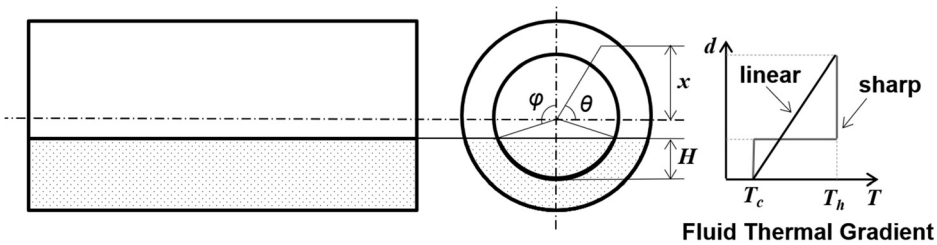

Fig. 9 Illustration of thermal stratification bending calculation with thermal gradient approximations to account for different mixing mechanisms

Note that the chemistry sampling flow from the hot leg loop drain is not expected to stratify, as a result of the current piping configuration that the sampling line is located fairly close to the vertical run of this drain line.

4.3 Thermal Stratification Induced Bending. Thermally stratified flow causes pipe to bend as a result of differential thermal expansion. Bending stress can be calculated based on similar assumption used in determining the stratification interface height, that is, the temperature change occurs right at the interface of the hot and cold fluid, corresponding to a sharp temperature gradient as illustrated in the diagram below. It is also assumed that the pipe wall shares the hot and cold temperatures, T_h and T_c, with the pipe fluid above and below the interface, respectively. On the other hand, the intermixing of hot and cold fluid over the entire cross section can be approximately estimated by a linear temperature gradient. The sharp temperature gradient is conservative as it results in the largest differential thermal expansion in the pipe axial direction as opposed to a linear thermal gradient across the full or partial pipe cross section.

To calculate the global bending of a pipe due to thermal stratification, the two temperature gradient profiles, as discussed earlier, are considered: a linear temperature gradient corresponding to a wide mixing and a step change corresponding to a narrow mixing of cold and hot fluid, as illustrated in Fig. 9, where the interface position is defined by angle ϕ and the interface height is denoted as H.

For the linear temperature gradient, the equivalent strain is exactly half of the thermal strain between the pipe inside and outside surfaces, therefore, the bending stress, $\sigma_b(x)$ at a given point with a distance of x from the neutral axis, and bending moment over the pipe cross section can be simply written as

$$\sigma_b(x) = \frac{1}{2}E(\alpha_c T_c - \alpha_h T_h)\cdot\frac{2x}{D} \tag{3}$$

$$M_{\text{linear}} = EI(\alpha_c T_c - \alpha_h T_h)\cdot\frac{1}{D} \tag{4}$$

For the sharp temperature gradient, the equivalent bending is calculated by considering the continuity and equilibrium equations at the pipe cross section, assuming fixed-end boundary condition, as follows:

$$\varepsilon_c - \varepsilon_h = \alpha_c T_c - \alpha_h T_h \tag{5}$$

$$E\varepsilon_c A_c + E\varepsilon_h A_h = 0 \tag{6}$$

Solve for ε_c, ε_h obtain

$$\varepsilon_c = \frac{\varphi}{\pi}(\alpha_c T_c - \alpha_h T_h) \tag{7}$$

$$\varepsilon_h = -\left(1 - \frac{\varphi}{\pi}\right)(\alpha_c T_c - \alpha_h T_h) \tag{8}$$

where ε_c, ε_h are thermal strains at the cold and hot sections of the pipe due to temperature difference and A_c, A_h are cross-sectional areas of the cold and hot sections, respectively. The equivalent bending moment due to thermal stratification is then calculated by integrating the equivalent bending strain over the pipe cross section

$$\begin{aligned} M_{\text{sharp}} &= \int\int E\varepsilon_c dA_c \cdot x + \int\int E\varepsilon_h dA_h \cdot x \\ &= \frac{2}{3}(R^3 - r^3)\sin\varphi \cdot E(\alpha_c T_c - \alpha_h T_h) \end{aligned} \tag{9}$$

where R and r are the outer and inner radius, respectively, of the pipe cross section. Thus, for a thin-walled pipe ($r \to R$), the equivalent bending stress and bending moment yield as

$$\sigma_b(x) = \left(\frac{2\sin\varphi}{\pi}\right)E(\alpha_c T_c - \alpha_h T_h)\cdot\frac{2x}{D} \tag{10}$$

$$M_{\text{sharp}} = \left(\frac{4\sin\varphi}{\pi}\right)EI(\alpha_c T_c - \alpha_h T_h)\cdot\frac{1}{D} \tag{11}$$

The bending stress formula for thin-walled pipe, derived herein, agrees with those reported in Refs. [11] and [12]. Note that a factor, K_{flex} accounting for the flexibility of the boundary conditions, can be added to the calculation. Considering the piping configuration and piping support characteristics, $K_{\text{flex}} = 1$ is set to conservatively represent the constraint condition. The thermal stratification bending moment at three temperature ranges (55, 189, and 244 °C), accounting for offline chemistry sampling, an intermediate temperature range, and online chemistry sampling, respectively, are included to investigate the effect of thermal stratification on fatigue damage.

4.4 Stress Analysis. The details of ASME class 1 piping stress method are provided in this section. As per ASME section

III [9], the alternating stress intensity is calculated by the equations below, provided that the primary plus secondary stress intensity or the thermal expansion stress and primary plus secondary membrane plus bending stress intensity criteria are met (NB-3653.6)

$$S_{\text{alt}} = K_e \frac{S_p}{2} \tag{12}$$

where S_p is the peak stress intensity range calculated as follows:

$$S_p = K_1 C_1 \frac{PD}{2t} + K_2 C_2 \frac{D}{2I} M_i + \frac{1}{2(1-v)} K_3 E\alpha |\Delta T_1| + K_3 C_3 E_{ab} |\alpha_a T_a - \alpha_b T_b| + \frac{1}{1-v} E\alpha |\Delta T_2| \tag{13}$$

K_e is the factor depending on the primary plus secondary stress intensity (of a given cycle) S_n, allowable design stress intensity S_m, and material parameters (m and n, provided in Table NB-3228.5(b)-1 [9]) by the following expression:

$$\begin{aligned} K_e &= 1.0, && S_n \le 3S_m \\ &= 1.0 + (1-n)/n(m-1)(S_n/3mS_m - 1), && 3S_m \le S_n < 3mS_m \\ &= 1/n, && S_n \ge 3S_m \end{aligned} \tag{14}$$

4.4.1 Thermal Stress. The peak stress intensity consists of primary stresses (membrane plus bending) and secondary stresses due to thermal gradients. ΔT_1 and ΔT_2 are the linear and nonlinear portion of the temperature range between outside and inside pipe surfaces, respectively, and are calculated as [9]

$$\Delta T_1 = \frac{12}{t^2} \int_{-t/2}^{t/2} yT(y)dy \tag{15}$$

$$\Delta T_2 = \max\left(|T_o - T| - \frac{1}{2}|\Delta T_1|, |T_i - T| - \frac{1}{2}|\Delta T_1|, 0 \right) \tag{16}$$

$$T = \frac{1}{t} \int_{-t/2}^{t/2} T(y)dy \tag{17}$$

where t is the pipe wall thickness, T_i and T_o are the pipe inside and outside temperatures, respectively, and $T(y)$ represent the temperature distribution across the pipe wall thickness. The TRHEAT computer code is used to determine the temperature responses of a pipe due to thermal transient in the contained fluid. A pipe is represented in TRHEAT as a slab of uniform thickness. The outside of the pipe is assumed to be insulated and the inside to be in contact with a fluid which undergoes a thermal transient. TRHEAT results include the equivalent linear and nonlinear pipe wall temperature gradients and the discontinuity temperature differences, required for calculation of piping stresses in accordance with the requirements for class 1 piping specified in the ASME boiler and pressure vessel code, section III, nuclear power plant components.

4.4.2 Stress Indices. The primary stress indices, B_1 and B_2, do not feed into the peak stress intensity calculations, rather, they determine the applicability of the calculation by the primary stress intensity criteria

$$B_1 \frac{PD}{2t} + B_2 \frac{D}{2I} M_i \le 1.5 S_m \tag{18}$$

C_1, C_2, and C_3 are secondary stress indices for specific component under investigation; K_1, K_2, K_3 are local stress indices for specific component under investigation. The stress indices given in Table NB-3681(a)-1 of Ref. [9], are applicable to girth fillet welds used to attach socket welding fittings, socket welding valves, slip-on flanges, or socket welding flanges. The primary stress indices, B_1 and B_2, and secondary stress indices, C_1 and C_2 for socket weld fittings shall be taken as follows:

$$\begin{aligned} B_1 &= 0.75(t_n/C_x) \ge 0.5 \\ B_2 &= 1.5(t_n/C_x) \ge 1.0 \\ C_1 &= 1.8(t_n/C_x) \ge 1.4 \\ C_2 &= 2.1(t_n/C_x) \ge 1.3 \end{aligned} \tag{19}$$

where t_n is the nominal pipe wall thickness and C_x is the fillet weld size. Bounding values of these stress indices can be calculated by using minimum fillet weld size (the minimum fillet weld size gives the maximum value of $t_n/C_x = 0.917$). The local stress indices K_1, K_2, K_3 and the other secondary stress indices C_3, C'_3 can be directly retrieved from Table NB-3681(a)-1 of Ref. [9]. The stress indices at the location of interest are summarized in Table 2 below. Note that it is the range of pressure, temperature, and moment between two load sets, which is to be used in the calculations. This calculation is based upon the effect of changes that occur in mechanical or thermal loadings which take place as the system goes from one load set to any other load set which follow it in time. The fatigue calculation is carried out at the DH line elbow within NUPIPE-II, which finds the most conservative load set for each transient analyzed to compute the alternating stress as well as other stress intensities and loading criteria associated with it. The thermal stratification bending moment is conservatively applied as an external load in the program.

4.5 Fatigue Calculation

4.5.1 Plant Operation and RCS Drain Line Transients. Transients from plant operations, such as plant heat-up and cooldown, can cause variations in pressure and thermal expansion to the RCS loop, which may also affect the loading condition of the RCS loop drain DH line elbow. However, to what degree these fluctuations in temperature and pressure would contribute to the loop drain line fatigue utilization highly depend on the piping configuration and pipe support constraints. Table 3 summarizes possible plant

Table 2 Stress indices for pipe elbow and welded sections

	Applicable for $D_0/t \le 100$ for C or K indices and $D_0/t \le 50$ for B indices								
	Internal pressure			Moment loading			Thermal loading		
Pipe products and joints	B_1	C_1	K_1	B_2	C_2	K_2	C_3	C'_3	K_3
Curved pipe or elbows, as specified within NUPIPE-II	1.000	1.256	1.000	1.466	1.954	1.000	1.000	0.500	1.000
Girth butt welds between nominally identical wall thickness items, as-welded	0.500	1.000	1.200	1.000	1.000	1.800	0.600	0.500	1.700
Girth fillet weld to socket weld, fittings, socket weld valves, slip on or socket welding flanges	0.688	1.376	3.000	1.651	1.927	2.000	2.000	1.000	3.000

Table 3 Plant operation transient conditions

Description of transients	Temperature range hot leg °F	Temperature range cold leg °F	Pressure range psi
Steady-state fluctuations	611–617	544–550	2200–2300
Plant loading	547–614	–	–
Reactor load increase/decrease	606–619	544–560	2155–2325
Reactor trip from full power	536–614	536–549	1870–2250
Pressurizer heatup/cooldown	70–547	70–547	400–2250
Large step decrease with steam dump	533–616	535–556	1975–2350
Loss of load from full power	551–640	547–580	1600–2500
Loss of flow one loop	499–620	507–547	1875–2250
Loss of power	547–634	546–558	2070–2500
Primary leak test	70–400	70–400	400–2250
Turbine test	475–547	475–547	1920–2250

transients along with the conditions and expected occurrence, estimated for the plant design life (NAPS technical records).

Thermal transients considered in this calculation are those due to RCS flow introduced through RCS loop drain DH lines during reactor coolant sampling and excess letdown. The reactor coolant sampling transients include online and offline sampling (conducted when reactor is online or offline) transients at the RCS loop drain lines off the hot leg and cold leg. It is considered that the reactor coolant temperatures of online sampling are plant normal operating temperatures of 319 and 286 °C (606 and 547±2 °F) for the hot and cold legs, respectively. The RCS flow temperature at offline condition (reactor shutdown) is considered to be 93 °C (200 °F). During the sampling transients, the RCS flow travels in the Loop Drain Line for a short section before exiting through the 20-mm (3/4 in.) sampling line. The excess letdown is only conducted at the cold leg, and the RCS flow travels through the entire loop drain line attached to the cold leg.

4.5.2 Cumulative Fatigue Usage Factor. The cumulative fatigue usage factor (CUF) is then calculated by summing up the individual fatigue usage factors for each pair of load cases as follows:

$$\mathrm{CUF} = \sum_{k=1}^{n} \frac{N_k}{N_{k,\,\mathrm{allow}}} \times 100\% \tag{20}$$

where N_k and $N_{k,\mathrm{allow}}$ are number of cycles and allowable number of cycles, respectively, of a given alternating stress intensity S_k. The allowable cycles can be interpolated logarithmically from the fatigue damage design curve for austenitic stainless steel in mandatory Appendix I of ASME boiler and pressure vessel code section III, division 1 [9], by using the following formula:

$$N_{k,\mathrm{allow}} = N_i \cdot \left(\frac{N_j}{N_i}\right)^{\left[\frac{\log\left(\frac{S_i}{S_{\mathrm{alt}}}\right)}{\log\left(\frac{S_i}{S_j}\right)}\right]} \tag{21}$$

where N_i and N_j, are allowable number of cycles at stress intensities S_i and S_j, found from the fatigue design curves, respectively. As CUF reaches 100% (also known as full utilization), it is considered that failure would occur in the materials or components being investigated.

5 Results and Discussions

The load cases corresponding to each transient, including the RCS loop drain transients and the plant transients, are paired within NUPIPE-II to produce maximum alternating stresses ranges. The plant transients are included to verify the impact on fatigue damage to the RCS loop drain line as a result of plant operation, such as pressurizer heat-up/cooldown, reactor load increase/decrease, and reactor trip from full power etc. (see Table 3). Note that the plant transients induce not only thermal loads but also primary loads due to pressure variations. To understand the thermal transient effect, two temperature change profiles were considered: a step change, where temperature increases instantaneously, and a ramp-to-plateau change, where temperature is ramped up linearly to the target temperature within a given time interval (measured). The linear and nonlinear thermal strain as a function of time is plotted for excess letdown transient condition in Fig. 10 for comparison. The rapid increase of thermal strain during excess letdown is due to the high flow volumetric velocity. The step change in temperature resulted in nearly 30% increase in peak strain as compared to that of the ramp-to-plateau change, which is based on measurement, thereby, more realistic. Thermal transient strain during chemistry sampling at the hot leg loop drain lines are shown in Fig. 11. For chemistry sampling, the thermal strain is much lower, and the transient curves are much flattened than that of the excess letdown, due to relatively low flow velocity. The step change and ramp-to-plateau change produced similar results in peak strain values.

Various transients, including plant operation transients and outflowing transients, are then investigated for their alternating stress intensities. Figure 12 presents a comparison for the RCS loop drain line DH elbow off the cold and hot leg, at the weld fitting upstream and downstream locations. No significant difference in stresses upstream and downstream of the weld fitting was noticed. The cold leg loop drain line sees slightly less stresses than hot leg because of lower operating temperature (by ~40 °C). It appears that the excess letdown produces the most severe thermal transient loads as compared to others. The online chemistry sampling is on the same level with the pressurizer cooldown, at about one third in

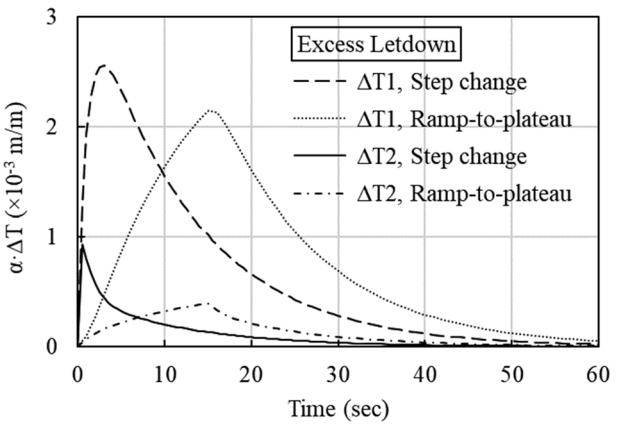

Fig. 10 Linear and nonlinear thermal strain as a function of time during Excess letdown thermal transient condition: Step change versus ramp-to-plateau change in temperature

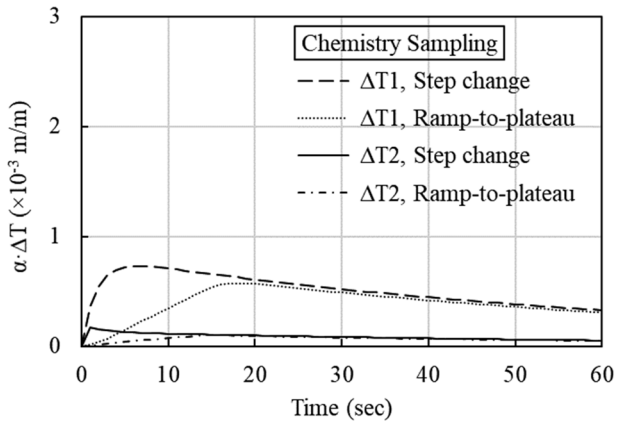

Fig. 11 Linear and nonlinear thermal strain as a function of time during chemistry sampling thermal transient condition: Step change versus ramp-to-plateau change in temperature

magnitude of that of the excess letdown transient. Other plant operation transients are at a much less magnitude in terms of alternating stress intensities.

To investigate thermal stratification induced damage, the alternating stress intensity of chemistry sampling transients with thermal stratification at various temperature ranges are plotted for comparison in Fig. 13. Different set of stress intensity indices were used to account for areas including the DH line elbow, butt-weld and socket-weld. The alternating stress intensities increase with increasing temperature ranges. The socket weld produces the highest stress intensity while the butt weld produces the lowest. The elbow section, using parameters for curved pipe, is also believed to induce stress concentration, and therefore, prone to flaw initiation. The stress intensity values for the socket weld and the elbow section increase significantly at the 244 °C temperature difference due to the increase of K_e factor as the primary plus secondary stress intensity exceeds $3S_m$.

These alternating stress intensities are translated to fatigue utilization and presented in Fig. 14. The worst-case scenario is the sharply stratified condition at the midsection with a socket weld fitting, which results in over utilization (failure) before 500 cycles are reached. At the stress level exceeding $3S_m$, the material undergoes plastic deformation, which accelerates the failure process, and a simplified elastic-plastic evaluation is triggered [9]. There had been concerns on the simplified elastic-plastic method being overly conservative, when the primary plus secondary stress range exceeds the limit of $3S_m$ [13,14]. However, we believe that a sharp-mixing thermal stratification is less likely to occur. Measurements suggest a wide-spread intermixing with temperature varying approximately linearly from top to bottom across the pipe is closer to the actual condition. Therefore, chemistry sampling with a linear stratified condition is considered realistic.

The cumulative utilization factors of the excess letdown, the online and offline chemistry sampling with thermal stratification, and various plant operation transients (combined), are presented

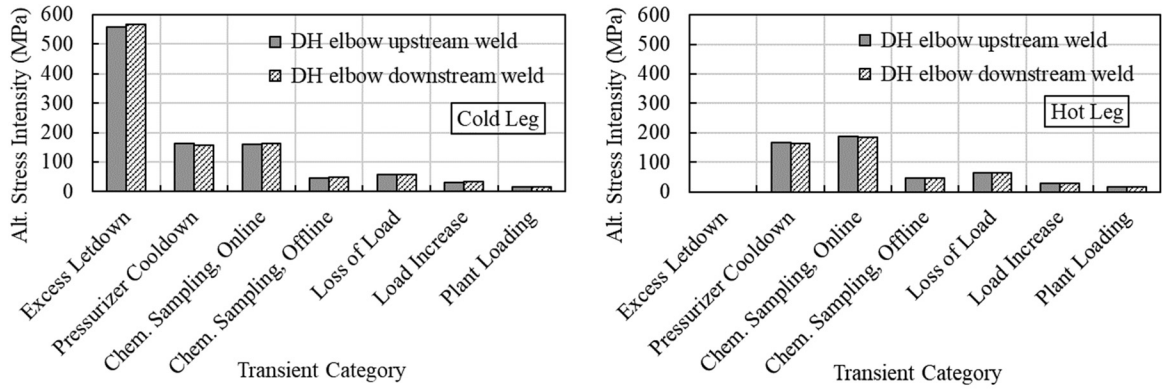

Fig. 12 Alternating stress intensity of RCS sampling transients at the weld fitting upstream and downstream locations of (*a*) cold leg and (*b*) hot leg RCS loop drain lines

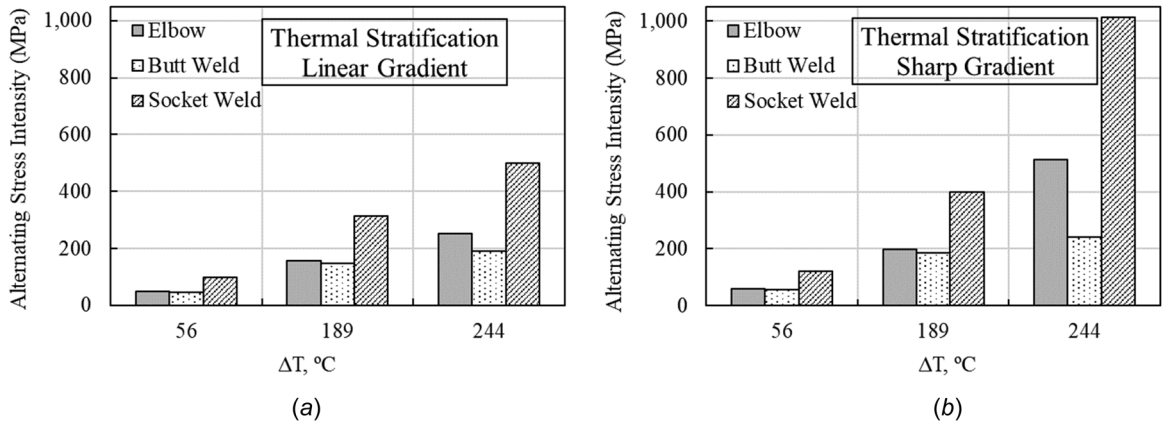

Fig. 13 Alternating stress intensity of RCS sampling transients with thermal stratification for DH line elbow, butt-welded, and socket-welded areas at various Δ*T*: (*a*) linear versus (*b*) sharp stratification gradient

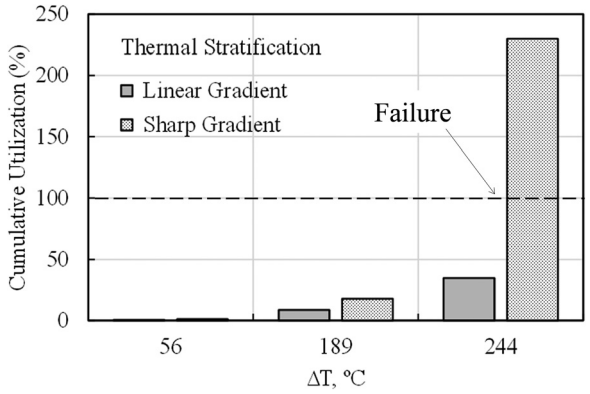

Fig. 14 Cumulative utilization factors as a result of thermal stratification during chemistry sampling activities for socket-welded areas at various ΔT: linear versus sharp stratification gradient

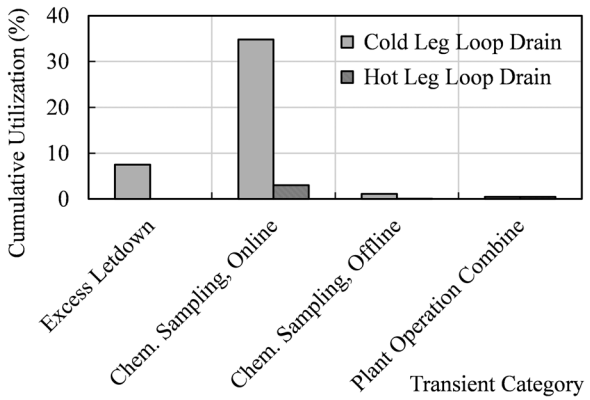

Fig. 15 Cumulative utilization factors of excess letdown, online and offline chemistry sampling, and combined plant operation transients for RCS loop drain lines off of cold and hot legs

for the RCS loop drain line DH elbows in Fig. 15. Only the results accounting for socket welds are presented, because of the most limiting stress values, which bound other cases. Noted that the elbow locations are bounding for all other areas identified as being susceptible in MRP-146 [2]. The offline sampling and plant operation transients, within the design limits and projected occurrences, have negligible effects on fatigue life of the piping. It appears that excess letdown is the most damaging transient to the RCS loop drain line because of high stress intensities as a result of large thermal expansion and rapid thermal transient condition. However, the cumulative fatigue damage from excess letdown is limited by its low occurrence with a CUF of ~8% at 80 cycles. For the chemistry sampling, though at less stress intensity, thermal stratification is expected to occur during this transient at the cold leg loop drain line and can cause severe damage to the DH elbow, depending on the flow intermixing conditions. The online chemistry sampling can cause a fatigue utilization of ~35%, within 10 years of operation at the current sampling frequency, assuming a linear thermal gradient over the pipe cross section. Altogether, the outflow activities may result in a fatigue utilization over 40% at the cold leg loop drain line. Keep in mind that this is in addition to damages from the swirl penetration, expected according to the current piping configuration. Therefore, the outflow activities are most likely responsible for the premature failure at the RCS cold leg loop drain line elbow. In comparison, the hot leg loop drain line only had a total fatigue utilization of less than 5%. This is consistent with the observation that cracks were only identified on the cold leg loop drain elbows.

As discussed earlier in this section, it is more realistic to apply the linear stratification bending moment, which is also supported by measurements from other lines at the North Anna power station. The sharp stratification is a worst-case scenario that is overly conservative, because (1) the hot and cold fluid usually intermix over a certain thickness; (2) the intermixing may not occur right at the center of the pipe cross section; and (3) the temperature difference may not be as high as the maximum temperature difference used in the calculation. These factors will reduce the actual thermal bending moment. However, the sharp stratification provides a bounding value from the analysis perspective.

6 Conclusions

The through-wall axial crack in the elbow region of the RCS "B" cold leg loop drain line at North Anna Power Station has been investigated for root causes through material inspection. The identified outflow transients along with plant operation transients were analyzed within the framework of ASME Class 1 piping formula. Together with analytical solutions to thermal stratification induced bending, we were able to quantitatively evaluate the severity of fatigue damaging effects for each transient. The findings and conclusions are summarized as follows:

(1) Material inspections through fractography using SEM imaging have suggested long exposure of the crack face in the RCS environment since the crack initiation and also confirmed thermal fatigue related failure mode during the crack propagation. Other degradation mechanisms, including stress corrosion cracking, general corrosion, and flow accelerated corrosion etc., have been ruled out by FMEA evaluation, which leads to investigation in possible additional damages from outflow activities.

(2) Plant operation transients, including plant heat-up and cooldown, pressurizer heat-up and cooldown, load increase and decrease, and loss of power, etc., have been combined using bounding temperature and pressure ranges in the fatigue evaluation and have shown negligible effects on fatigue of the RCS loop drain lines, with a CUF less than 1% over the plant entire design life.

(3) Outflow activities, particularly the excess letdown and chemistry sampling while plant is online can cause significant fatigue damage to the RCS loop drain lines: the excess letdown induces high thermal stress from its large thermal expansion and rapid transient condition. However, the cumulative fatigue damage from excess letdown is limited by its low occurrence; the online chemistry sampling can cause a fatigue utilization of ~35% at the RCS cold leg loop drain line within 10 years of operation at the current sampling frequency, as thermal stratification is expected to occur. Altogether, the outflow activities may result in a fatigue utilization over 40%, which is in addition to damages as expected from the swirl penetration. In contrast, the offline chemistry sampling has negligible damaging effects if the coolant temperature is kept below 93 °C (200 °F) during the process.

(4) It is realistic to apply the linear stratification bending moment, which is supported by measurements from other lines at the station. The sharp stratification is a worst-case scenario that is overly conservative. However, it provides a bounding value from the analysis perspective.

With the above conclusions, we have made the following recommendations for plant operation: given the damage conditions and overall unknowns regarding stratification effects on fatigue, if on-line sampling is performed or excess letdown is placed in service, ultrasonic testing examination in accordance with MRP-146 guidance shall be performed on the affected loop drain line(s). The outflow examination is not required for Hot Leg loop drains, given that: (1) the fatigue utilizations was shown to be less than 1, conservatively calculated based on reasonable thermal stratification assumptions, for the current licensing basis period and (2) any additional online sampling will not result in significant damages. Evaluations performed for offline sampling (RCS

temperature $\leq 93\,^{\circ}\mathrm{C}$ or $200\,^{\circ}\mathrm{F}$) have demonstrated that there is no significant fatigue usage resulting from sampling while the unit is offline, and no ultrasonic examinations are required following normal outage sampling.

Acknowledgment

This work is sponsored by Dominion Energy, Inc., under internal funding from capital projects. The authors give special thanks to Dominion Energy Corporate Material Testing Group for their support on material inspections, as well as the station engineers for providing valuable data and insights.

Funding Data

- Dominion Energy, Inc. (No. 54-1229715).

Nomenclature

A_c = pipe cross section area in cold condition, m^2
A_h = pipe cross section area in hot condition, m^2
A_y = stratified flow area defined by critical depth, m^2
$B_{1,2}$ = primary stress indices
C_x = fillet weld size, m
$C_{1,2,3}$ = secondary stress indices
d = inside diameter of a pipe, m
D = outside diameter of a pipe, m
E = elastic modulus, MPa
E_{ab} = elastic modulus for dissimilar materials, MPa
E_c = elastic modulus at cold temperature, MPa
E_h = elastic modulus at hot temperature, MPa
g = gravitational acceleration, $\mathrm{m{\cdot}s}^{-2}$
H = stratified flow interface height, m
I = area moment of inertia, m^4
K_e = factor for alternating stress intensity
$K_{1,2,3}$ = local stress indices
M_i = resultant range of moment, N·m
M_{linear} = bending moment due to linear stratification, N·m
M_{sharp} = bending moment due to sharp stratification, N·m
$N_{i,j}$ = allowable number of cycles from fatigue design curves
N_k = number of cycles of a given stress intensity
$N_{k,\mathrm{allow}}$ = allowable number of cycles of a given stress intensity
P = pipe pressure range, MPa
Q = volumetric flow rate, $\mathrm{m}^3{\cdot}\mathrm{s}^{-1}$
r = inside radius of a pipe, m
R = outside radius of a pipe, m
$\mathrm{Ri_p}$ = Richardson number
$S_{i,j}$ = alternating stress intensity from fatigue design curve, MPa
S_m = allowable design stress intensity, MPa
S_n = primary plus secondary stress intensity, MPa
S_p = peak stress intensity, MPa
S_{alt} = alternating stress intensity, MPa
t = pipe wall thickness, m
T = pipe mean temperature across wall thickness, K
t_n = nominal pipe wall thickness, m
T_i = pipe inside temperature, K
T_o = pipe outside temperature, K
W_y = width of stratified flow free surface, m
x = distance from a given point to neutral axis, m
y = distance from a given point to the center, m
y_c = critical depth, m
α = thermal expansion coefficient, $(\mathrm{m/m}){\cdot}\mathrm{K}^{-1}$
α_c = thermal expansion coefficient at cold temperature, $(\mathrm{m/m}){\cdot}\mathrm{K}^{-1}$
α_h = thermal expansion coefficient at hot temperature, $(\mathrm{m/m}){\cdot}\mathrm{K}^{-1}$
α_y = angle bounding the critical depth, radian
$\Delta\rho$ = density difference between stratified fluids, $\mathrm{kg{\cdot}m}^{-3}$
ΔT_1 = linear portion of temperature range, K
ΔT_2 = nonlinear portion of temperature range, K
ν = Poisson's ratio
ρ = density of flowing fluids, $\mathrm{kg{\cdot}m}^{-3}$
σ_b = bending stress, MPa
φ = angle defining position of stratification interface, radian

Acronyms

ASME = American Society of Mechanical Engineering
CUF = cumulative fatigue usage factor
DH = down horizontal
EPRI = Electric Power Research Institute
FMEA = failure modes and effect analysis
ID = inside diameter
MRP = material reliability program
NAPS = North Anna Power Station
NRC = Nuclear Regulatory Commission
OE = operating experience
OD = outside diameter
PWR = pressurized water reactor
RCP = reactor coolant pump
RCS = reactor coolant system
SEM = scanning electron microscope
SG = steam generator
SPS = Surry power station

References

[1] Electric Power Research Institute, 2004, *Materials Reliability Program: Thermal Cycling Screening and Evaluation Model for Normally Stagnant Non-Isolable Reactor Coolant Branch Line Piping With a Generic Application Assessment*, Electric Power Research Institute, Palo Alto, CA, Standard No. MRP-132

[2] Electric Power Research Institute, 2005, *Materials Reliability Program: Management of Thermal Fatigue in Normally Stagnant Non-Isolable Reactor Coolant System Branch Lines*, Electric Power Research Institute, Palo Alto, CA, Standard No. MRP-146.

[3] Electric Power Research Institute, 2006, *EPRI Thermal Fatigue Evaluation per MRP-146, Version 1.0*, Electric Power Research Institute, Palo Alto, CA, Standard No. MRP-170.

[4] Electric Power Research Institute, 2009, *Materials Reliability Program: Management of Thermal Fatigue in Normally Stagnant Non-Isolable Reactor Coolant System Branch Lines Supplemental Guidance*, Electric Power Research Institute, Palo Alto, CA, Standard No. MRP-146S.

[5] McDevitt, M., 2015, *Industry Response to Recent Thermal Fatigue Operating Experiences*, NRC-Industry Material Workshop, Washington, DC, accessed Nov. 1, 2021, https://sanonofresafety.files.wordpress.com/2015/06/10-thermal-fatigue-update.pdf

[6] Seo, Y. H., Youm, H. K., and Jin, T. E., 2003, "Fatigue Effect of RCS Branch Line With Thermal Stratification," Proceedings of 11th International Conference on Nuclear Engineering, Tokyo, Japan, Apr. 20–23, Paper No. ICONE11-36541.

[7] Kweon, H. D., Kim, J. S., and Lee, K. Y., 2008, "Fatigue Design of Nuclear Class 1 Piping Considering Thermal Stratification," Nucl. Eng. Des., **238**(6), pp. 1265–1274.

[8] Dahlberg, M., Nilsson, K. F., Taylor, N., Faidy, C., Wilke, U.,Chapuliot, S., Kalkhof, D., Bretherton, I., Church, M., Solin, J., and Catalano, J., 2011, "Development of a European Procedure for Assessment of High Cycle Thermal Fatigue in Light Water Reactors: Final Report of the NESC-Thermal Fatigue Project," *European Commission and Directorate-General Joint Research Centre Institute for Energy*, Petten, The Netherlands, Report No. EUR-22763-EN.

[9] ASME, 2010, "Rules for Construction of Nuclear Facility Components, Division 1, Subsection NB, Class 1 Components," American Society of Mechanical Engineering (ASME) Boiler and Pressure Vessel Code, Section III, Division 1, New York.

[10] Electric Power Research Institute, 1999, "Thermal Stratification, Cycling, and Striping (TASCS)," Electric Power Research Institute, Palo Alto, CA, Report No. TR-103581.

[11] Talja, A., and Hansjosten, E., 1990, "Results of Thermal Stratification Tests in a Horizontal Pipeline at the HDR-Facility," Nucl. Eng. Des., **118**(1), pp. 29–41.

[12] Schuler, X., and Herter, K. H., 2004, "Thermal Fatigue Due to Stratification and Thermal Shock Loading of Piping," 30th MPA-Seminar in Conjunction With the Ninth German-Japanese Seminar, Stuttgart, Germany, Oct. 6–7, pp. 6.1–6.16.

[13] Zeng, L., Jansson, L. G., and Dahlstrom, L., 2010, "On Fatigue Verification of Class 1 Nuclear Power Piping According to ASME NB-3600," 18th International Conference on Nuclear Engineering, Xi'an, China, May 17–21, Paper No. ICONE18-29049, pp. 375–383.

[14] Gurdal, R., and Xu, S. X., 2009, "A Comparative Study of K_e Factor in Design by Analysis for Fatigue Evaluation," ASME Paper No. PVP2008-61222.